



# The electrical properties of a fullerene and C.I. Acid Red 2 (methyl red) doped E7 nematic liquid crystal

M. Okutan<sup>a</sup>, S.E. San<sup>a,\*</sup>, O. Köysal<sup>b</sup>, E. Şentürk<sup>c</sup>

<sup>a</sup> Department of Physics, Gebze Institute of Technology, Gebze, 41400 Kocaeli, Turkey

<sup>b</sup> Department of Physics, Çanakkale Onsekiz Mart University, 17100 Çanakkale, Turkey

<sup>c</sup> Department of Physics, Sakarya University, 54100 Sakarya, Turkey

## ARTICLE INFO

### Article history:

Received 24 June 2009

Received in revised form

31 August 2009

Accepted 6 September 2009

Available online 17 September 2009

### Keywords:

Liquid crystals

Fullerene-C<sub>60</sub>

Dielectric constant

Conductivity

Activation energy

Hopping conduction

## ABSTRACT

The electrical properties of a C.I. Acid Red 2 (4-dimethylaminoazobenzene-2'-carboxylic acid) and fullerene mixture of the nematic liquid crystal E7 were studied using complex dielectric spectroscopy as a function of the frequency of the applied AC–DC signal at various temperatures. Both the real and imaginary components of the dielectric constant decreased with increased frequency of the applied field whilst the AC conductivity increased with increasing frequency of the applied field. The alternating current conductivity  $\sigma(\omega)$  varied with angular frequency,  $\omega$  as  $\omega^s$ , with  $s \leq 1$ , suggesting that a dominant hopping conduction process operated. The temperature dependence of both the AC conductivity and the exponent  $s$  can be reasonably well interpreted using a correlated barrier hopping model.

© 2009 Elsevier Ltd. All rights reserved.

## 1. Introduction

Liquid Crystal (LC) based materials have received much attention owing to their manifold electronic and medical applications [1–3]. Polymer dispersed liquid crystal (PDLC) systems have also proven popular due to their application in electro-optics, such as optical switches, reflective displays without polarizer and switchable windows [4]. Valuable discussions of the mechanism of doped LC systems have been published [5,6]; in this context, E7 is a eutectic mixture which has been widely studied in PDLC materials as it offers a wide range of operating temperatures for use in display devices, privacy windows, optical shutters and light valves [7–10]. Polymer/E7 mixtures, such as poly(n-butylacrylate), poly(styrene), poly(methylmethacrylate) etc. have also been reported [4–19].

In dielectric spectroscopy (DS), which can be used to determine molecular detail, [20], alternating current conductivity (AC) measurements are used to characterize the electrical properties of materials. These measurements have attracted attention because they can provide information about conduction mechanisms [21].

This work concerns a polymer/E7 mixture based, hybrid LC structure, comprising 4-dimethylaminoazobenzene-2'-carboxylic acid (C.I. Acid Red 2; MR) and a fullerene-C<sub>60</sub> dispersion of E7. The dielectric and AC–direct current (DC) electrical conductivity of the MR/C<sub>60</sub>/E7 mixture was determined over the frequency range 1 k–1 M Hz with a temperature variation of 300–380 K.

## 2. Experimental work

The measurement cell comprised two glass slides separated by Mylar sheets of ~8 µm thickness. Before the construction of the cells, Indium tin oxide (ITO) covered glass substrates were spin coated with polyvinyl alcohol (PVA) at 2000 rpm and cured at 323 K for ~2 h. The thickness of the coating was ~100 nm; the coating layers were rubbed, unidirectionally, with velvet so as to obtain preliminary molecular orientation. The ultimate form of the constructed cell was planar with 2° of rubbing tilt. C<sub>60</sub> was dissolved in toluene and the toluene fraction evaporated to eliminate fullerene powder. The chemical formulas of the dye, fullerene and the nematic host are shown in Fig. 1. A LC, was doped with 0.5% MR and comprising 0.5% by mass C<sub>60</sub> in E7, was prepared.

The AC conductivity and the dielectric properties were analyzed from the capacitance and the conductance values at some different temperatures. The Hewlett-Packard 4194A Impedance Analyzer

\* Corresponding author. Fax: +90 262 6051304.

E-mail address: [erens@gyte.edu.tr](mailto:erens@gyte.edu.tr) (S.E. San).

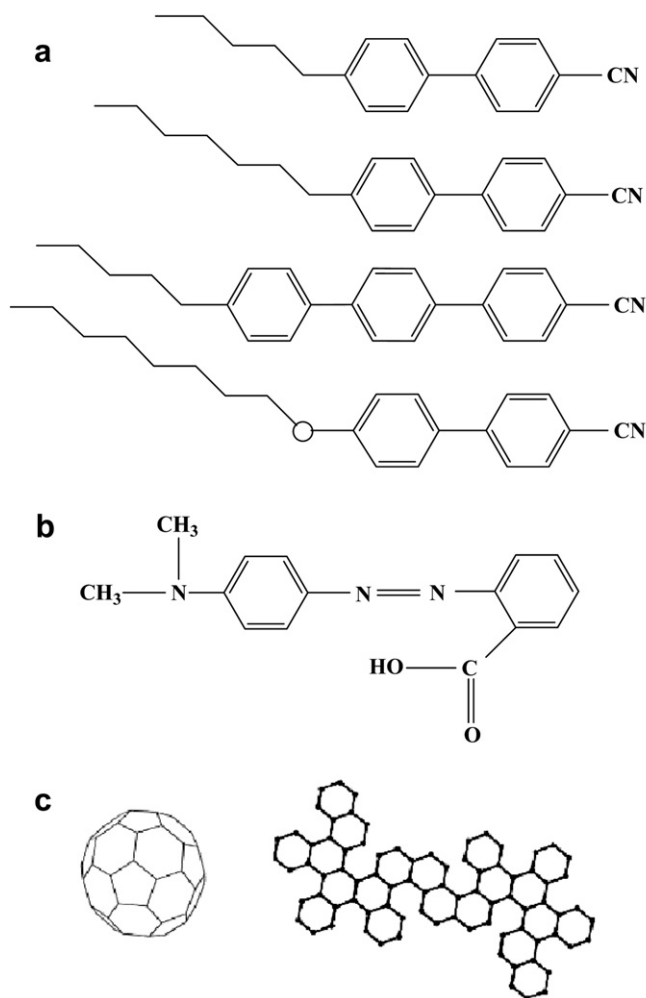


**Fig. 1.** Chemical formulas of: (a) nematic host, E7, (b) '4-dimethylaminoazobenzene-2'-carboxylic acid', MR, (c) fullerene, C<sub>60</sub>.

was utilized during these measurements. The complex dielectric response was reported between 1 k and 1 M Hz. The rms amplitude of the device is  $\sim 495$  mV. The temperature was controlled by using a PT 100 resistor, which is in direct thermal contact with the sample. It could be monitored between 300 and 380 K with accuracy better than 0.1 K by using NOVOTERM Temperature Control System. The AC dielectric properties were analyzed from the capacitance and the conductivity values in the temperature range of 300–380 K. The sample was heated to higher temperatures and at a fixed temperature, more than 30 frequencies were applied. The time for one frequency sweep at a fixed temperature was approximately 1 min. For each single temperature point, the real and imaginary parts of dielectric permittivity as well as time, temperature and frequency were recorded in a personal computer.

### 3. Results and discussion

The real part of the dielectric constant was calculated from the equation  $\epsilon' = Cd/(\epsilon_0 A)$ , where  $\epsilon_0$  is the permittivity of the free space,  $d$  is the inter-electrodes distance. The dielectric loss  $\epsilon''$  was calculated from the equation  $\epsilon'' = \epsilon' \tan(\delta)$ , where  $\delta = 90 - \varphi$  and  $\varphi$  is the phase angle. As seen from Fig. 2a, the real part of dielectric constant  $\epsilon'$  initially decreases rapidly with the increase in frequency as frequency increases  $\epsilon'$  attains a constant value. The decrease in  $\epsilon'$  with frequency can be attributed to the fact that, at low frequencies,

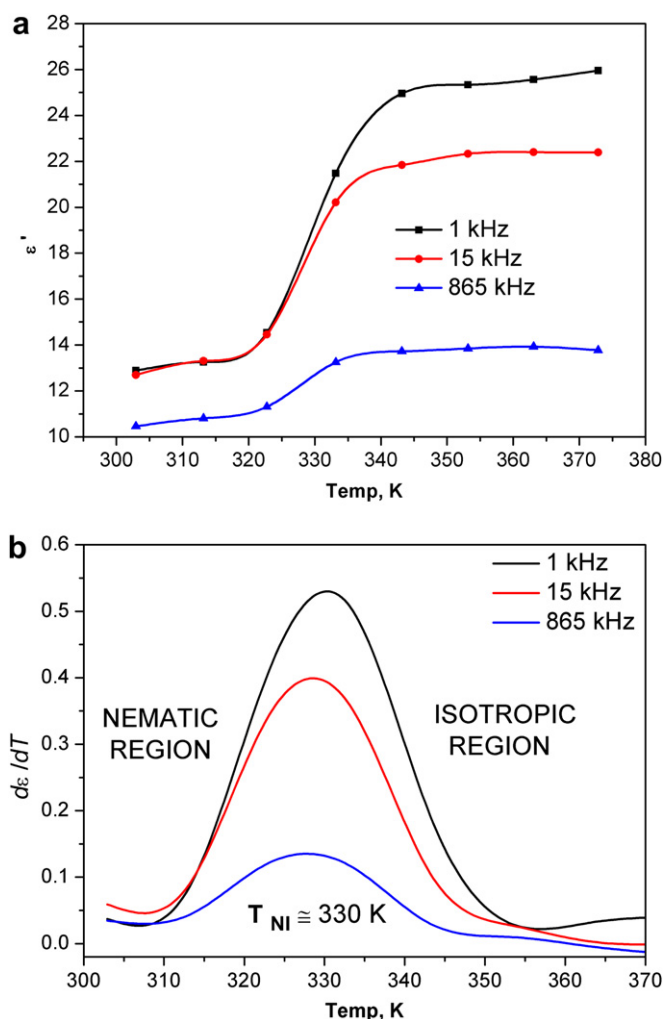


**Fig. 2.** a) Temperature dependency of the real part of the dielectric constant at various frequencies, b) differential variation of dielectric constant with respect to temperature.

$\epsilon'$  for polar materials depends on the contribution of multi components of polarizability, deformational (electronic and ionic) and relaxation (orientational and interfacial) polarization. The former polarizability depends on the electrons and ions while the latter depends on orientational or interfacial effects. The increase in frequency leads to a decrease in the orientational polarization, since this takes more time than electronic and ionic polarization do. Such a decrease tends to reduce the value of  $\epsilon'$  with increasing frequency, reaching a constant value at higher frequency [22].

In mentioned temperature interval above, not only the real part of the dielectric constant but also conductivity plots of the sample exhibit one anomaly at  $\sim 330$  K. This anomaly corresponds probably to a structural phase transition, which transforms liquid crystal from the nematic to isotropic ( $T_{NI}$ ) as shown in Fig. 2b. The increase of the temperature in the nematic phase and its rapid change at the transition to the isotropic state show that this process is strongly affected by the nematic potential. The dielectric constant value changed suddenly at  $\sim 330$  K might be related to continuous release of the reorientation of the dipole groups [5]. Moreover, the temperature dependency of differential dielectric constant shows that the phase transition is first order.

Actually, the same trend was observed for the imaginary part of the dielectric constant. Fig. 3 shows the temperature dependency of  $\epsilon''$  at various frequencies. The same anomaly can be seen for the

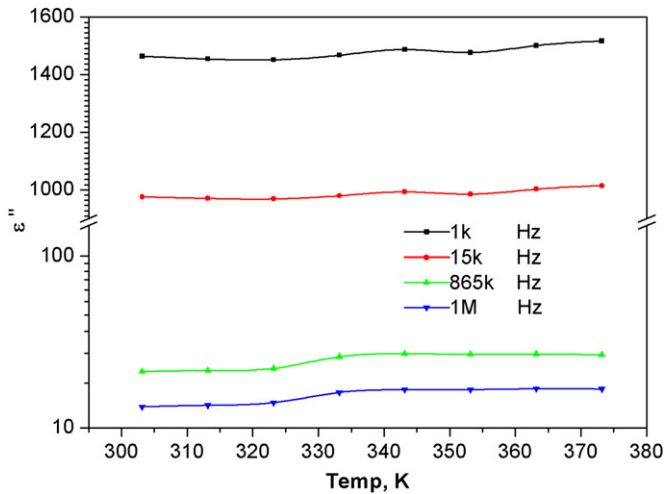


Fig. 3. Temperature dependency of the imaginary part of the dielectric constant at various frequencies.

imaginary part at  $\sim 330$  K. Moreover, the observed behavior may be attributed to the single relaxation process in mentioned frequency interval [23].

The AC conductivity,  $\sigma(\omega)$  of the film was also measured as a function of frequency at some stabilized temperatures. Fig. 4 exhibits the frequency dependencies of the cell at different temperatures on a log–log scale. The conductivity shows strong frequency dependency at low temperatures. This frequency dependent conductivity peculiarity can be analyzed using a universal power law;

$$\sigma(\omega, T) = \sigma_{DC}(T) + A(T)\omega^{s(T)} \quad (1)$$

where  $A$  is the complex constant,  $\omega$  is the angular frequency ( $\omega = 2\pi f$ ). As seen from Fig. 4, it is observed that the frequency dependence of conductivity shows two distinct regimes, within the measured frequency window, (i) the low frequency DC plateau region (lower than 100 kHz) and (ii) high frequency dispersion region. Plateau region corresponds to frequency independent conductivity  $\sigma_{DC}(T)$ . Its value is obtained by extrapolating the conductivity to the zero frequency.

Fig. 5 shows temperature dependence of the DC conductivity. As the temperature increases, the transition from the DC plateau to AC

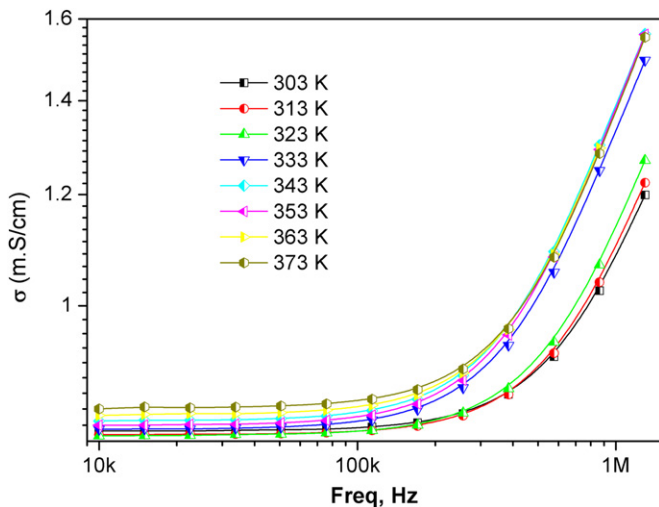


Fig. 4. Frequency dependency of AC conductivity at some stabilized temperatures.

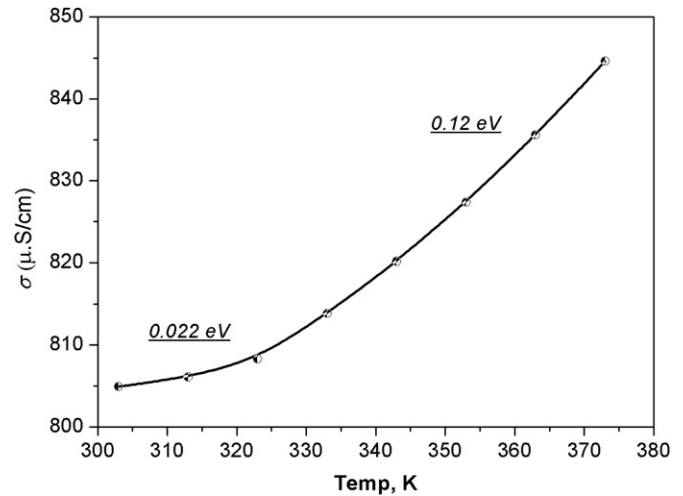


Fig. 5. Plot of the DC conductivity at various temperatures.

conductivity dispersion region shifts towards higher frequencies. Dispersion region is characterized by the random hopping of mobile ions. Exponential dependence of the measured conductivity on temperature indicates the applicability of another well-known expression for conductivity [5];

$$\sigma_{DC}(T) = \sigma_{01} \exp\left(-\frac{E_{Nem}}{k_B T}\right) + \sigma_{02} \exp\left(-\frac{E_{Iso}}{k_B T}\right) \quad (2)$$

where  $E_{Nem}$  and  $E_{Iso}$  are activation energies of the mobile charge carriers in nematic and isotropic state,  $k_B$  is Boltzmann constant and  $\sigma_{01}$  and  $\sigma_{02}$  are pre-exponential factors. At lower temperatures, a slight deviation from the custom behavior of conductivity has been noticed. The values of the activation energies are determined from the slope of the  $\ln \sigma_{DC}$  conductivity versus  $1000/T$ . The activation energies of the material have been estimated to be 0.12 eV at high temperatures  $\sim 330$ – $380$  K and 0.022 eV at low temperatures  $\sim 300$ – $330$  K. It is well known that, at least two transport mechanisms are considered when a change is observed in the slope of the DC conductivity, (see Fig. 5). One of these mechanisms is a transport, which is by carriers excited beyond a mobility edge into extended states leading to an activated energy at high temperatures. The other is the hopping of carriers between localized states near the Fermi energy at lower temperatures [24].

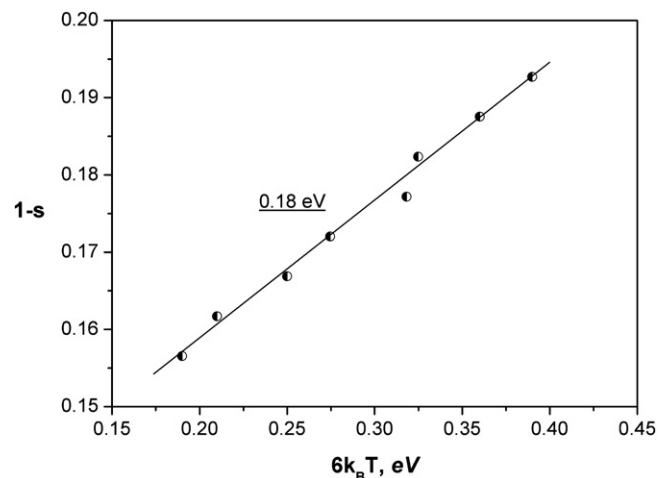


Fig. 6. Temperature dependency of  $s$  parameter with respect to activation energy.

The index  $s$  has values less or very close to unity and it is found to vary with temperature in this work. The values of frequency exponent were derived from the slope of the curves in Fig. 4 assuming a linear dependence of  $\log \sigma$  on  $\log w$  over the relevant frequency range and deriving the slope from a linear regression analysis. The temperature dependence of  $s$  is illustrated in Fig. 6. The exponent  $s$  has values decreasing with increasing temperatures. So we can say that our results of the temperature dependence of  $s$  and its range of values (0.79–0.61) are consistent with the correlated barrier hopping (CBH) model of [25–27]. In this model, thermally activated hopping of the charge carriers is proposed for two localized sites over the energy separating barrier [28]. The expression for  $s$  is derived on the basis of this model and is given by [27] as,

$$s = 1 - \frac{6k_B T}{W_M - k_B T \ln(1/w\tau_0)} \quad (3)$$

where  $k_B$  is the Boltzmann constant,  $T$  is the absolute temperature in Kelvin and  $W_M$  is the maximum barrier height. Here  $\tau_0$  is the characteristic relaxation time and is at the order of  $\tau_0 \sim 10^{-13}$  s [27]. For large value of  $W_M/k_B T$ ,  $s$  is near unity. Also above equation predicts that  $s$  decreases with increasing temperature at large  $W_M/k_B T$ . The above demonstrations lead to the approach of [22,27].

$$s = 1 - \frac{6k_B T}{W_M} \quad (4)$$

where  $W_M$  is the optical band gap of MR/C<sub>60</sub>/E7. The slope of Fig. 6 leads us to calculate the optical band gap energy  $W_M$  for the MR/C<sub>60</sub>/E7 sample. The calculated value of barrier height  $W_M$  is found to be 0.18 eV.

#### 4. Conclusions

The measurements have been carried out at the temperature range 300–380 K and in the frequency range 1 k–1 M Hz. The electrical conductivity and dielectric plots of MR/C<sub>60</sub>/E7 exhibit one anomaly which corresponds probably to a structural phase transition from the nematic to isotropic phase at  $T_{NI} \cong 330$  K. Phase transitions' intensity is also found to be frequency dependent. The AC conductivity was found to increase with increasing frequency according to the power law  $\sigma \propto w^s$  and exponent value  $s$  decreased with increasing temperature. We have observed that temperature

dependency of DC conductivity is not linear. Activation energies at the DC analyze of the LC has been found to be 0.12 eV at isotropic region and 0.022 eV at nematic region respectively. The values of  $s$  range from 0.71 to 0.69 in mentioned temperature interval and the optical band gap is found to be 0.18 eV. It was found that the CBH model is appropriate for explaining the frequency and temperature dependencies of the AC conductivity and its frequency exponent.

#### References

- [1] Richards C, Tiddy GJT, Casey S. *Colloids and Surfaces A: Physicochemical and Engineering Aspects* 2006;288:103–12.
- [2] Kayacan O, San SE, Okutan M. *Physica A – Statistical Mechanics and Its Applications* 2007;377(2):523–30.
- [3] Judele R, Laschat S, Baro A, Nimtz M. *Tetrahedron* 2006;62:9681–7.
- [4] Cho YH, Kawade R, Kubota T, Kawakami Y. *Science and Technology of Advanced Materials* 2005;6:435–42.
- [5] Okutan M, San SE, Basaran E, Yakuphanoglu F. *Physics Letters A* 2005;339:461–5.
- [6] Bedjaoui L, Gogibus N, Ewen B, Pakula T, Coqueret X, Benmouna M, et al. *Polymer* 2004;45:6555–60.
- [7] Drzaic PS. *Liquid crystal dispersions*. Singapore: World Scientific; 1995.
- [8] Higgins DA. *Advanced Materials* 2000;12:251.
- [9] Maschke U, Benmouna M, Coqueret X. *Macromolecular Rapid Communications* 2002;23:159.
- [10] Mucha M. *Progress in Polymer Science* 2003;28:837.
- [11] Okutan M, Köysal O, San SE. *Displays* 2003;24:81–4.
- [12] Zhou J, Petti L, Mormile P, Roviello A. *Optics Communications* 2004;231:263–71.
- [13] Cho D, Yang G. *Journal of Luminescence* 2006;117:199–208.
- [14] Senyurt Askim F, Warren Garfield, Whitehead Jr Joe B, Hoyle Charles E. *Polymer* 2006;47:2741–9.
- [15] San SE, Okutan M, Köysal O, Ono H, Kawatsuki N. *Optics Communications* 2004;238:79–84.
- [16] Allwood DA, Dyer PE, Gonzalo J, Snelling HV, Hird M. *Chemical Physics Letters* 1999;301:91–7.
- [17] Patnaik SS, Pachter R. *Polymer* 1999;40:6507–19.
- [18] Almeida PL, Tavares S, Martins AF, Godinho MH, Cidade MT, Figueirinhas JL. *Optical Materials* 2002;20:97–100.
- [19] Kim BK, Cho YH, Lee JS. *Polymer* 2000;41:1325–35.
- [20] Okutan M, Yakuphanoglu F, San SE, Köysal O. *Physica B* 2005;368:308–17.
- [21] Okutan M, Basaran E, Bakan HI, Yakuphanoglu F. *Physica B* 2005;364:300–5.
- [22] Farid AM, Atiyah HE, Hegab NA. *Vacuum* 2005;80:284–94.
- [23] Okutan M, Şentürk E. *Journal of Non-Crystalline Solids* 2008;354(14):1526–30.
- [24] Aydogdu Y, Erol I, Yakuphanoglu F, Aydogdu A, Ahmedzade M. *Synthetic Metals* 2003;139:327–34.
- [25] Shaaban MH, Ali AA, El-Nimr MK. *Materials Chemistry and Physics* 2006;96:433–8.
- [26] Özer M, Altındal A, Özkaya AR, Bulut M, Bekaroğlu Ö. *Synthetic Metals* 2005;155:222–31.
- [27] El-Barry AMA, Atiyah HE. *Physica B* 2005;368:1–7.
- [28] Şentürk E, Okutan M, San SE, Köysal O. *Journal of Non-Crystalline Solids* 2008;354(30):3525–8.